Impedance Tuning with Notched Waveforms for Spectrum Sharing in Cognitive Radar

Angelique Dockendorf[1], Austin Egbert[1], Adam Goad[1], Caleb Calabrese[1], Benjamin Adkins[1], Brandon Ravenscroft[2], Jonathan Owen[2], Charles Baylis[1], Shannon Blunt[2], Anthony Martone[3], Kyle Gallagher[3], and Robert J. Marks II[1]

[1]Baylor University, Waco, TX, USA
[2]University of Kansas, Lawrence, KS, USA
[3]Army Research Laboratory, Adelphi, MD, USA

***Abstract*—In a congested radio spectrum, radar systems must be capable of sharing spectrum in real time. Two possible radar transmission approaches involve either avoiding interferers or placing a notch in the sub-bands of interference. Impedance tuning allows the radar transmitter power amplifier to maximize its output power while adjusting its linearity to meet notch and/or out-of-band spectral requirements. In real-time spectrum sharing, the system controller decides whether to provide a waveform that notches around the interference or to avoid the interference altogether. Considerations in this decision include the maximum detection range obtainable from a tuned amplifier versus the finest achievable range resolution, based on transmitted bandwidth. This paper describes a comparison of real-time impedance tuning for notched, random FM waveforms versus a contiguous-band chirp used for avoidance. Comparisons are made between the range (calculated from output power) and the range resolution (calculated from bandwidth) obtained by the optimized circuits in these two cases.**

***Keywords*—cognitive radar, power amplifiers, radio spectrum management, notched waveforms, spectrum sharing**

I. Introduction

The re-allocation of radar S-band spectrum for sharing with wireless communications is only the most recent example of an ongoing trend that is driving research on radar spectrum sharing [1-7]. One method of sharing is for the radar to transmit in a contiguous band of frequencies that changes based on the radio frequency interference (RFI) gleaned from the environment. In such scenarios, a tunable matching network can be placed after the transmitter power-amplifier device and tuned in real-time to operate between the RFI frequencies [8]. Real-time tuning of the amplifier is useful because the output power, the power-added efficiency (PAE), and the adjacent-channel power ratio (ACPR) of an amplifier all depend on the load impedance presented to the amplifier [9], which is also affected by changing antenna impedance due to mutual coupling in arrays [10]. Real-time circuit tuning under control of a cognitive radio platform can therefore improve output power in frequency/beam agility scenarios. Kirk [11] likewise demonstrates the use of a software-defined radio (SDR) platform to maximize bandwidth, signal-to-interference-plus-noise ratio (SINR), and target-to-clutter ratio for spectrum sharing by sensing the spectrum, and then choosing the band for transmission.

In some sharing scenarios, rather than change the contiguous band of operation, spectral notches [12-15] can be placed within the transmitted radar bandwidth at the particular sub-bands occupied by RFI. A recent approach has relied upon the inherent maneuver freedom of random FM waveforms [16] to incorporate notches. Specifically, Jakabosky [17] demonstrates Tukey windowing to taper the range sidelobes otherwise induced by sharp notch edges, and Mohr [18] uses a spectral frequency-template error (FTE) metric for optimization of notched waveforms. Ravenscroft [19] provides an holistic perspective on the use of notched random FM waveforms for radar detection in an environment with stationary and dynamic RFI, integrating this approach into a cognitive radio platform using a perception-action cycle for spectrum sensing, decision making, and adaptation. Valette [20] subsequently discusses the interaction of notched waveforms with power amplifier nonlinearities.

In [21] Semnani demonstrates a 90 W evanescent-mode (EVA) cavity impedance tuner that provides the capability to reconfigure within hundreds of milliseconds by adjusting the positions of discs atop its two cavities, with loss of only ~0.75 dB across most of the Smith Chart. This tuner is likewise shown by Alcala-Medel [8] to be frequency-agile over the S-band radar allocation using fast tuning algorithms developed by Dockendorf [22]. Here we demonstrate the use of this cavity tuner to perform impedance tuning for spectrally notched waveforms, providing the capability to optimize the power amplifier nonlinearities to obtain desirable notch depth and out-of-band spectral performance while maximizing the radar range.

II. Measurement Results: Impedance Tuning Implications on the Decision to Notch or Avoid

With the availability of notched waveforms (e.g. [12-19]), a cognitive radar may either notch around RFI frequencies or avoid the interference by selecting a smaller contiguous bandwidth. The impedance tuning considerations contribute to an engineering trade-off that must be negotiated between these two operating conditions. If a "notch" decision is made, the matching circuit can be tuned to maximize the power under the stringent consideration of meeting the sharp notch roll-off. If nonlinearities in the power amplifier cause intermodulation that fills the notch, then the load impedance must be tuned to focus on linearizing the amplifier device rather than improving the output power. As such, the greater bandwidth available from the notched waveform, and accompanying improvement in

range resolution, might come at a sacrifice of output power and a related undesirable decrease in radar range.

In performing experiments to investigate the trade-off between range and range resolution for the "notch" and "avoid" cases, the Baylor research team performed measurements on two versions of notched random FM from the University of Kansas, which inherently possess constant amplitude. Because their generation involves spectral shaping optimization, both to ensure good spectral roll-off in the out-of-band region and to initiate spectral notches, the deployment-ready version of each waveform exists in a discretized form that must be appropriately implemented as a continuous waveform in hardware. For example, [24] discusses the process required to realize spectrally notched waveforms on the modest fidelity available on an SDR platform.

For high-fidelity implementations such as can be achieved with an arbitrary waveform generator (AWG) it is necessary to up-sample the waveform to the DAC rate of the AWG. However, if these waveforms are sinc-interpolated when up-sampling, which would seem to be the obvious approach, significant amplitude modulation (AM) in the time-domain can arise. Consequently, AM to phase modulation (AM-PM) nonlinearities in the power amplifier can cause spectral spreading, thus resulting in significant degradation of notch depth [23].

On the other hand, constant amplitude can be preserved by performing interpolation solely in the phase domain. As such, AM-PM conversion does not become an issue, and impedance tuning can be used to maximize output power rather than being traded to improve linearity and thereby maintain notch depth.

We shall herein show two examples of using real-time impedance tuning with notched waveforms for radar applications. The trade-off between range and range resolution is examined for sinc-interpolated (non-constant modulus) and phase-interpolated (constant-modulus) notched waveforms. The benefit of using phase-interpolated waveforms is confirmed through these experiments to benefit both range and range resolution.

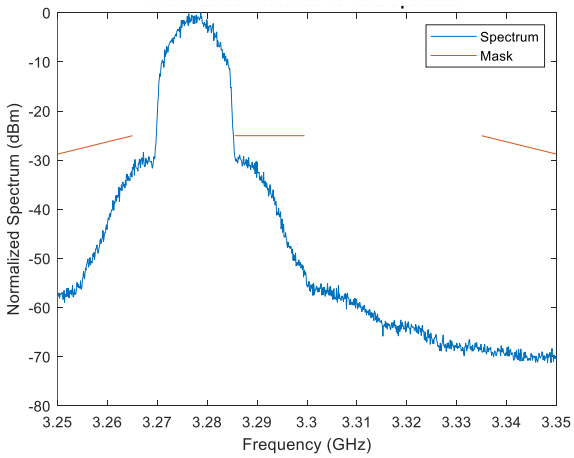

Fig. 1. Random FM contiguous-band waveform with 15 MHz bandwidth: "avoid low" case

A. Sinc-Interpolated Notched Waveforms

A simplified spectrum sharing scenario is constructed involving an overall bandwidth of 60 MHz at a center frequency of 3.3 GHz (3.27 – 3.33 GHz). RFI having 15 MHz bandwidth is assumed to reside within the sub-band between 3.285 and 3.3 GHz (i.e. 15 MHz from the lower end of the band and 30 MHz from the upper end). Consequently, the cognitive radar controller has three options to operate without interference: "avoid low", "avoid high", or "notch". A comparison of these three options based on best performance obtainable through impedance tuning is examined.

Figure 1 shows the "avoid left" possibility, where a contiguous-band random FM waveform is synthesized to be lower than the 15 MHz RFI (indicated by the center red line). Likewise Fig. 2 shows the "avoid high" possibility where a contiguous-band random FM waveform is synthesized higher than the RFI. This case achieves a wider bandwidth than Fig. 1 because there is more available spectrum as specified by the mask. Finally, Fig. 3 shows a notched random FM waveform that has been sinc-interpolated, thus realizing a notch depth of about 30 dB. Clearly, a notched waveform provides more total bandwidth than the avoidance-based waveforms, thereby providing better range resolution, because it can make use of the available spectrum on both sides of the RFI.

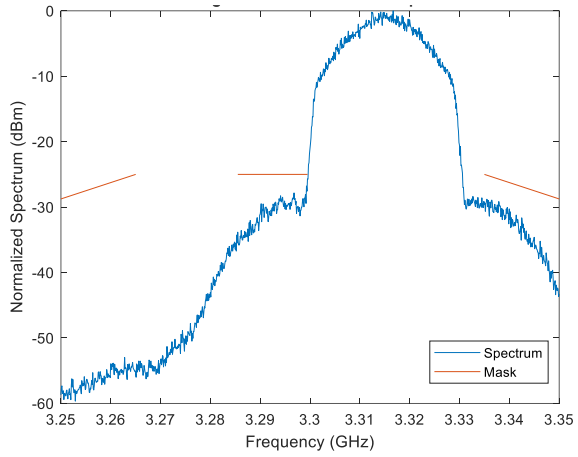

Fig. 2. Random FM contiguous-band waveform with 30 MHz bandwidth: "avoid high" case

For each of these waveforms and their corresponding spectral mask, a full load-pull measurement was performed using the Purdue University Generation 2 EVA cavity tuner over the combinations of the two cavity position numbers (n_1, n_2) [25]. Figures 4, 5, and 6 show the load-pull measurement results for the "avoid low", "avoid high", and "notch" cases, respectively. The output power contours are shown, along with a shaded region representing the range of (n_1, n_2) combinations for which the spectral mask is violated. Table I delineates the maximum constrained output power and detectable range for each waveform, as well as the calculated approximate range resolution based on the bandwidth of the waveform.

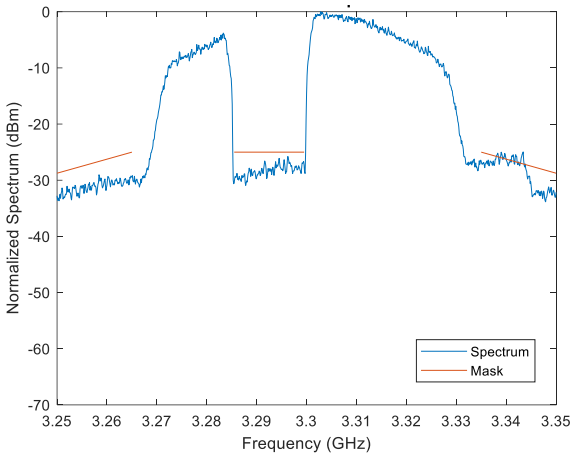

Fig. 3. Random FM waveform over 60 MHz band containing a 15 MHz notch

TABLE I: CONSTRAINED OPTIMUM VALUES FOR AVOID AND NOTCH CASES AT CONSTRAINED OPTIMUM LOAD IMPEDANCE

Waveform	Max (n_1, n_2)	Max P_{out} (dBm)	S_m (dB)	Max. Range (km)	Range Res. (m)
Avoid Low	(3424, 3925)	17.95	–2.74	16.9	18.20
Avoid High	(3124, 3975)	18.13	–0.07	17.0	9.10
Sinc-Interp. Notched	(3674, 3925)	17.57	–0.25	16.5	4.40

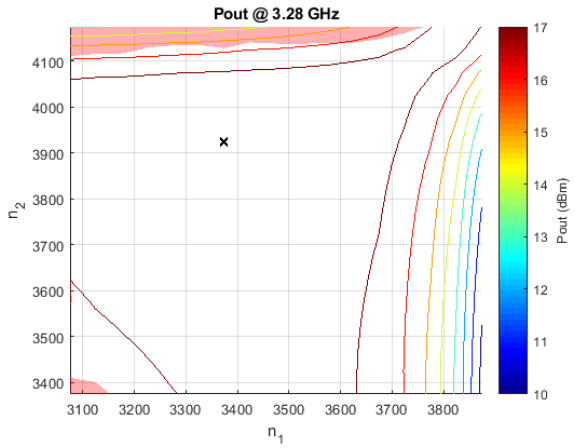

Fig. 4. Output power load-pull measurement results in tuner cavity position number combinations (n_1, n_2) for the "avoid low" waveform of Fig. 1. The region causing violation of the spectral mask is shaded.

Figure 6 shows that the sinc-interpolated implementation of the notched, random FM waveform causes very little of the (n_1, n_2) plane to be available for impedance matching. As such, the constrained optimum P_{out} is much lower than the global optimum. While the contours look similar in all three cases, the two "avoid" cases in Figs. 4 and 5 show a greater spectrally acceptable region of the (n_1, n_2) plane, which results in higher constrained optimum P_{out}. Of course, sinc-interpolation is not the appropriate way to implement a notched waveform on a AWG because, as noted earlier, doing so introduces AM that invalidates the transmitter-ready FM nature.

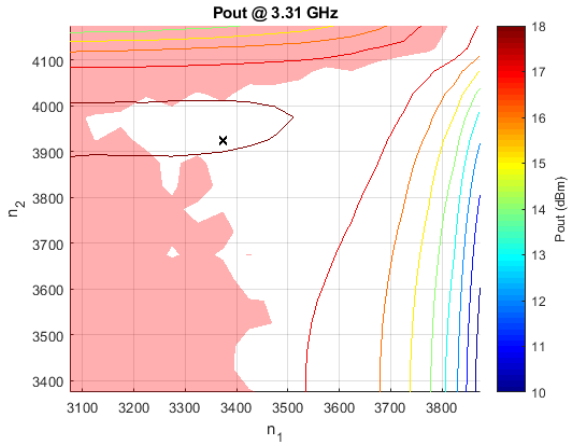

Fig. 5. Output power load-pull measurement results in tuner cavity position number combinations (n_1, n_2) for the "avoid high" waveform of Fig. 2, with the constrained optimum shown with 'x'. The region causing violation of the spectral mask is shaded.

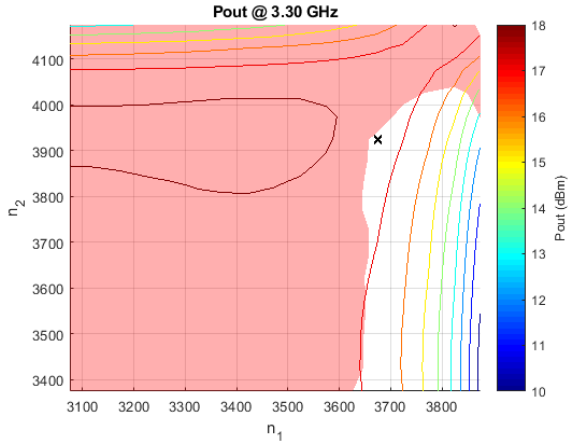

Fig. 6. Output power load-pull measurement results in tuner cavity position number combinations (n_1, n_2) for the notched, sinc-interpolated random FM waveform of Fig. 3, with the constrained optimum shown with 'x'. The region causing violation of the spectral mask is shaded.

B. Phase-Interpolated Notched Waveforms

In contrast to the sinc-interpolated implementation considered above, now consider a phase-interpolated implementation that preserves constant amplitude (per [19]). Consequently, the possibility of AM-PM conversion from amplifier nonlinearities is eliminated. Figure 7(a) shows the normalized spectrum for a phase-interpolated random FM waveform, with and without an amplifier terminated in an impedance resulting in significant nonlinearities. For comparison, Fig. 7(b) shows the sinc-interpolated waveform for the same conditions.

The former case, where the contant amplitude is preserved, realizes negligible difference with or without the amplifier in Fig. 7(a). This result is expected because, by maintaining the FM structure, the waveform is well-suited to a high power amp. Alternatively, the sinc-interpolated case in Fig. 7(b) shows roughly 20 dB of degradation in notch depth due to the distortion that is ultimately caused by AM imposed on the signal that translates into AM-PM nonlinearity in the amplifier.

Simply put, the even seemingly innocuous details of the implementation become quite important when high power and high fidelity are both required.

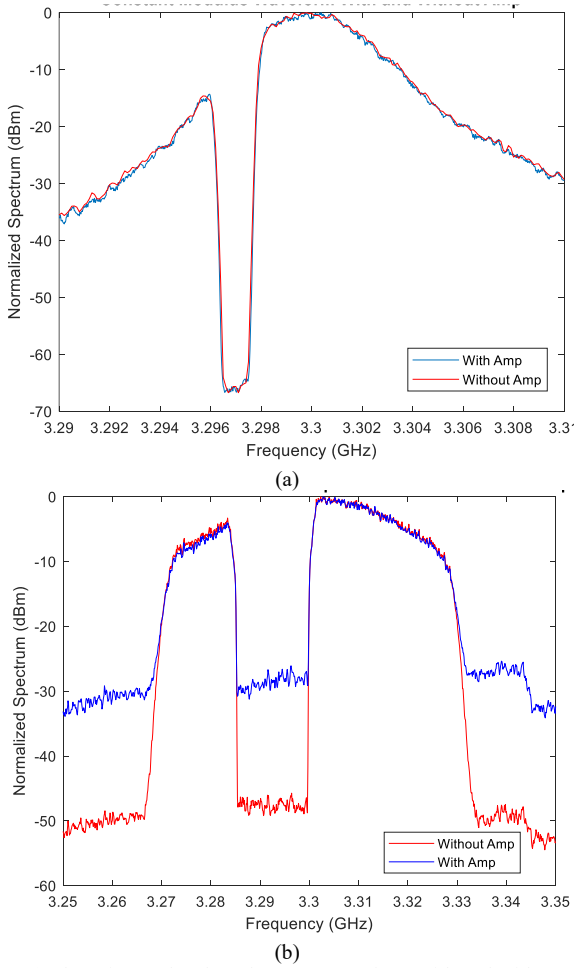

Fig. 7. (a) Phase-interpolated random FM waveform with and without power amplifier and (b) sinc-interpolated random FM waveform with and without power amplifier. Both waveforms were measured at the same tuner (n_1, n_2) setting (same load impedance).

Figures 8 and 9 compare use of an "avoid high" LFM chirp and a notched, random FM waveform (phase-interpolated), respectively, to determine the best range and range resolution that can be obtained given a set of spectral constraints that dictate the out-of-band roll-off and avoidance of a 1 MHz RFI source (with acceptable transmit power of –57 dBm). Here the former case has a 6 MHz bandwidth to (mostly) achieve the desired spectral constraints, while the latter employs all of the available 20 MHz, aside from the 1 MHz notch. Further, the LFM does not meet the RFI avoidance criterion, while the notched waveform achieved the required notch depth with room to spare.

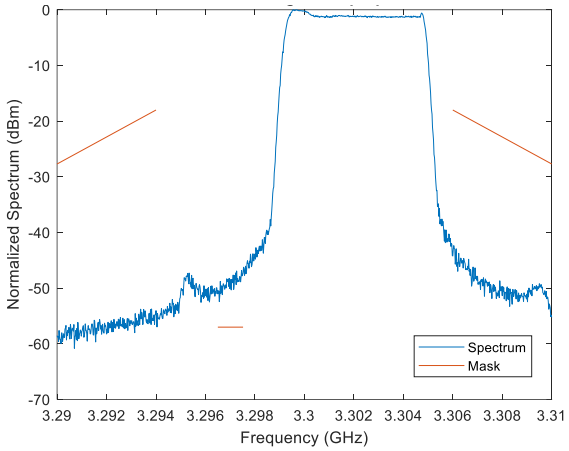

Fig. 8. "Avoid right" chirp for a 1 MHz notch and –57 dBm depth enforcement

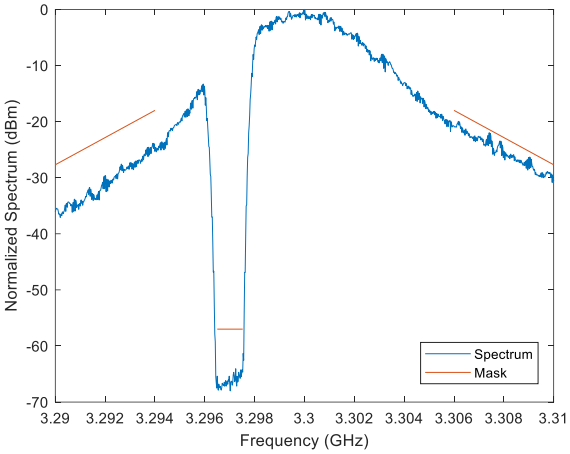

Fig. 9. Random FM waveform with a 1 MHz notch and –57 dBm depth enforcement

Figures 10 and 11 show the output power load-pull contours for the waveforms in Figs. 8 and 9, respectively. The power of the "avoid" chirp must be reduced to meet the depth enforcement aspect of the mask for the 1 MHz RFI. The load-pull result for this waveform (Fig. 10) shows a maximum output power of approximately 4 dBm. However, Fig. 11 shows a maximum output power of approximately 18 dBm for the notched waveform (phase-interpolated), with the entire (n_1, n_2) plane meeting spectral requirements.

Table II depicts a comparison of the search results between the "notch" and "avoid" cases for the scenario above. A range of 16.91 km is available with the notched, random FM waveform, while only 7.91 km of range is available with the "avoid" chirp waveform at the optimum output power load impedance. Additionally, the notched waveform provides finer range resolution due to the use of all available bandwidth.

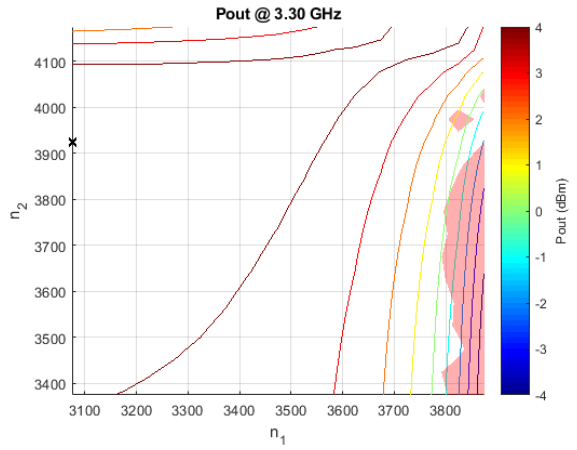

Fig. 10. Output power load-pull measurement results tuner cavity position number combinations (n_1, n_2) for the "avoid left" waveform of Fig. 8 after a power back-off is performed, allowing the waveform the possibility of meeting notch-depth spectral mask criteria. The constrained optimum is shown with 'x', and the region causing violation of the spectral mask is shaded.

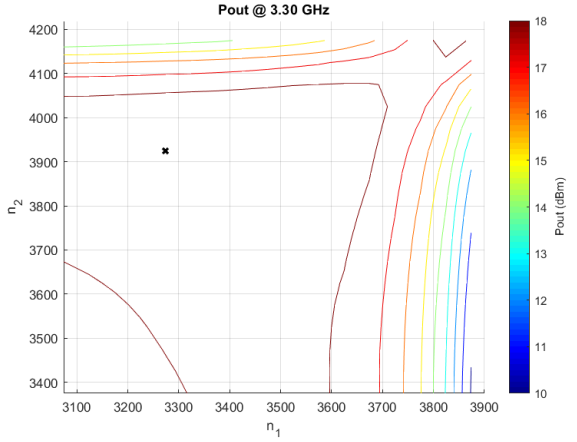

Fig. 11. Output power load-pull measurement results tuner cavity position number combinations (n_1, n_2) for the notched, constant-modulus PRO-FM waveform of Fig. 9. The constrained optimum is shown with 'x', and the entire viewable region is spectral-mask compliant.

TABLE II: CONSTRAINED OPTIMUM VALUES FOR AVOID AND NOTCH CASES AT CONSTRAINED OPTIMUM LOAD IMPEDANCE

Waveform	Max (n_1, n_2)	Max P_{out} (dBm)	S_m (dB)	Max. Range (km)	Range Res. (m)
Avoid High	(3074, 3925)	4.79	–2.05	7.91	285.03
Phase-Interp. Notched	(3274, 3925)	17.99	–0.47	16.91	121.35

III. CONCLUSIONS

An investigation has been presented on the impact of impedance tuning upon the decision of whether to use a notched waveform or contiguous-band waveform when a cognitive radar is contending with in-band RFI. The implementation of (discretely) optimized waveforms on an AWG also plays an important role, with standard sinc-interpolation leading to rather significant degradation due to AM-PM amplifier nonlinearities that necessitate power back-off to compensate. In contrast, phase-interpolation preserves the FM structure of the waveform, thereby avoiding these AM-PM effects altogether. Consequently, both range and range resolution can be optimized through impedance tuning without fear of inducing undesired spreading into the notch. These results are critical in integrating amplifier limitations into cognitive-radar decision making where notching or avoidance of RFI is required.

ACKNOWLEDGMENT

This work has been funded by the Army Research Laboratory (Grant No. W911NF-16-2-0054 and W911NF-15-2-0063). The views and opinions expressed do not necessarily represent the opinions of the U.S. Government. The authors are grateful to John Clark of the Army Research Laboratory for assistance in development of this paper.

REFERENCES

[1] J.M. Peha, "Sharing spectrum through spectrum policy reform and cognitive radio," *Proc. IEEE*, vol. 97, no. 4, pp. 708-719, Apr. 2009.

[2] S. Bhattarai, J. Park, B. Gao, K. Bian, W. Lehr, "An overview of dynamic spectrum sharing: ongoing initiatives, challenges, and a roadmap for future research," *IEEE Trans. Cognitive Communications & Networking*, vol. 2, no. 2, pp. 110-128, June 2016.

[3] F. Sanders, J. Carroll, G. Sanders, R. Sole, R. Achatz, L. Cohen, "EMC measurements for spectrum sharing between LTE signals and radar receivers," NTIA Technical Report TR-14-507, July 2014.

[4] FCC Rulemaking 12-354: "3.5 GHz band / citizens broadband radio service," available at www.fcc.gov/wireless/bureau-divisions/broadband-division/35-ghz-band/35-ghz-band-citizens-broadband-radio.

[5] FCC Notice DA 15-131, "Auction of advanced wireless services (AWS-3) licenses closes," Jan. 2015.

[6] Cisco white paper, "Cisco visual networking index: global mobile data traffic forecast update, 2016–2021," 28 Mar. 2017.

[7] S.D. Blunt, E.S. Perrins, *Radar & Communication Spectrum Sharing*, SciTech Publishing, 2018.

[8] J. Alcala-Medel, A. Egbert, C. Calabrese, A. Dockendorf, C. Baylis, G. Shaffer, A. Semnani, D. Peroulis, A. Martone, E. Viveiros, R.J. Marks II, "Fast frequency-agile real-time optimization of high-power tuning network for cognitive radar applications," *IEEE MTT-S Intl. Microwave Symp.*, Boston, MA, June 2019.

[9] J. Sevic, K. Burger, M. Steer, "A novel envelope-termination load-pull method for ACPR optimization of RF/microwave power amplifiers," *IEEE MTT-S Intl. Microwave Symp. Digest*, vol. 2, pp. 723-726, June 1998.

[10] J.L. Allen, "Gain and impedance variation in scanned dipole arrays," *IRE Trans. Antennas & Propagation*, vol. 10, no. 5, pp. 566-572, Sept. 1962.

[11] B.H. Kirk, J.W. Owen, R.M. Narayanan, S.D. Blunt, A.F. Martone, K.D. Sherbondy, "Cognitive software defined radar: waveform design for clutter and interference suppression," *Proc. SPIE Defense & Security,* vol. 10188, Radar Sensor Technology XXI, Anaheim, CA, May 2017.

[12] J.R. Guerci, S.U. Pillai, "Adaptive transmission radar: the next 'wave'?", *IEEE National Aerospace & Electronics Conf.*, Dayton, OH, Oct. 2000.

[13] I.W. Selesnick, S.U. Pillai, "Chirp-like transmit waveforms with multiple frequency-notches," *IEEE Radar Conf.*, Kansas City, MO, May 2011.

[14] C. Nunn, L.R. Moyer, "Spectrally compliant waveforms for wideband radar," *IEEE Aerospace & Electronic Systems Mag.*, vol. 27, no. 8, pp. 11-15, Aug. 2012.

[15] A.W. Doerry, J.M. Andrews, S.M. Buskirk, "Digital synthesis of linear-FM chirp waveforms: comments on performance and enhancements," *SPIE Defense & Security,* vol. 9077, Radar Sensor Technology XVIII, Baltimore, MD, May 2014.

[16] S.D. Blunt, J.K. Jakabosky, C.A. Mohr, P.M. McCormick, J.W. Owen, et al., "Principles & applications of random FM radar waveform design," to appear in *IEEE Aerospace & Electronic Systems Magazine*.

[17] J. Jakabosky, B. Ravenscroft, S.D. Blunt, A. Martone, “Gapped spectrum shaping for tandem-hopped radar/communications & cognitive sensing,” *IEEE Radar Conf*., Philadelphia, PA, May 2016.

[18] C.A. Mohr, P.M. McCormick, S.D. Blunt, C. Mott, "Spectrally-efficient FM noise radar waveforms optimized in the logarithmic domain," *IEEE Radar Conf*., Oklahoma City, OK, Apr. 2018.

[19] B. Ravenscroft, J.W. Owen, J. Jakabosky, S.D. Blunt, A.F. Martone, K.D. Sherbondy, "Experimental demonstration and analysis of cognitive spectrum sensing & notching," *IET Radar, Sonar & Navigation*, vol. 12, no. 12, pp. 1466-1475, Dec. 2018.

[20] A. Valette, M. Ariaudo, S. Traverso, I. Fijalow, L. Zerioul, “Robustness of filter bank multicarrier signals to power amplifier nonlinearities,” *46th European Microwave Conf*., London, UK, Oct. 2016.

[21] A. Semnani, M. Abu Khater, D. Peroulis, C. Baylis, L. Hays, C. Kappelmann, Z. Hays, “An evanescent-mode cavity-based high-power impedance tuner for adaptive radar applications,” *USNC-URSI National Radio Science Meeting*, Boulder, CO, Jan. 2018.

[22] A. Dockendorf, A. Egbert, E. Langley, C. Calabrese, J. Alcala-Medel, S. Rezayat, Z. Hays, C. Baylis, A. Martone, E. Viveiros, K. Gallagher, A. Semnani, D. Peroulis, “Fast optimization algorithm for evanescent-mode cavity tuner optimization and timing reduction in software-defined radar implementation, submitted to *IEEE Trans. Aerospace & Electronic Systems*.

[23] A. Dockendorf, A. Goad, C. Calabrese, B. Adkins, A. Egbert, J. Owen, B. Ravenscroft, C. Baylis, R.J. Marks II, S. Blunt, A. Martone, K. Sherbondy, E. Viveiros, “The impact of nonlinear power amplifier load impedance on notched waveforms for cognitive radar spectrum sharing,” *IEEE Radio & Wireless Symp*., San Antonio, TX, Jan. 2020.

[24] C.A. Mohr, J.W. Owen, S.D. Blunt, C.T. Allen, “Zero-order reconstruction optimization of waveforms (ZOROW) for modest DAC rates,” submitted to *IEEE Intl. Radar Conf.*, Washington, DC, Apr. 2020.

[25] A. Semnani, G.S. Shaffer, M.D. Sinanis, D. Peroulis, “High-power impedance tuner utilising substrate-integrated evanescent-mode cavity technology and external linear actuators,” *IET Microwaves, Antennas & Propagation*, vol. 13, no. 12, pp. 2067-2072, Oct. 2019.